

# Synchrotron spectroscopy of confined carriers in CdF<sub>2</sub>-CaF<sub>2</sub> superlattices

K. V. Ivanovskikh,<sup>1,2</sup> R. B. Hughes-Currie,<sup>1</sup> M. F. Reid,<sup>3,4</sup> J.-P. R. Wells,<sup>4,a)</sup> N. S. Sokolov,<sup>5</sup> and R. J. Reeves<sup>3,4</sup>

<sup>1</sup>Department of Physics and Astronomy, University of Canterbury, PB 4800, Christchurch 8140, New Zealand

<sup>2</sup>Institute of Physics and Technology, Ural Federal University, Ekaterinburg 620002, Russia

<sup>3</sup>MacDiarmid Institute for Advanced Materials and Nanotechnology, P.O. Box 600, Wellington 6140, New Zealand

<sup>4</sup>Dodd-Walls Centre for Photonic and Quantum Technologies and Department of Physics and Astronomy, University of Canterbury, PB4800, Christchurch 8140, New Zealand

<sup>5</sup>Ioffe Physical-Technical Institute, Russian Academy of Sciences, 194021 St. Petersburg, Russia

(Received 17 November 2015; accepted 25 February 2016; published online 14 March 2016)

Luminescence spectroscopic and temporal dynamic properties of high energy elementary excitations in CdF<sub>2</sub>-CaF<sub>2</sub> superlattices have been studied utilising excitation with vacuum ultraviolet and X-ray synchrotron radiation while comparing the results with those obtained for CdF<sub>2</sub> and CaF<sub>2</sub> bulk crystals. It is shown that the optical properties of the superlattice structures are determined by exciton emission in the CdF<sub>2</sub> monolayers. The experimental manifestations of exciton confinement phenomena are discussed. © 2016 AIP Publishing LLC.

[<http://dx.doi.org/10.1063/1.4943498>]

## I. INTRODUCTION

Semiconductor quantum wells were first proposed in the early 1960s and experimentally realised in the 1970s,<sup>1</sup> remaining the subject of extensive investigation over the last four decades, see for example, Refs. 2–5. Typically, these works are motivated by the interesting and often unique optical properties which can be obtained, leading to applications in spintronics or lasers for example. By contrast, interest in very thin heterostructures comprised of alternating layers of insulating dielectric materials (such as CaF<sub>2</sub>) has been far more recent (dating from the 1990s<sup>6–9</sup>) and made possible by the progress in nanofabrication achieved by researchers working on inorganic semiconductor materials.

In this work, we focus on vacuum ultraviolet (VUV) spectroscopy of CdF<sub>2</sub>-CaF<sub>2</sub> superlattices. Superlattices (SLs) are structures formed by a periodic combination of monolayers (ML) of materials having different band gaps, thereby representing a sequence of quantum wells and barriers with modified optical properties. In particular, confinement effects are expected to be noticeable for SLs with monolayers of a few nanometers where critical dimensions are comparable to typical electron wavelengths or migration range of mobile electronic excitations (excitons, electrons). Therefore, it is important to investigate the spectroscopy and dynamics of relaxation of intrinsic electronic excitations in SLs that may provide a more comprehensive picture of the electronic processes in nanoscale insulating optical materials.

CdF<sub>2</sub> and CaF<sub>2</sub> are characterised by the same fluorite-type cubic crystal structure with similar lattice constants making them suitable for superlattice growth; however, their electronic and optical properties differ significantly. Most notably and in spite of its large band gap of about 8 eV, appropriately co-doped and annealed CdF<sub>2</sub> can have n-type

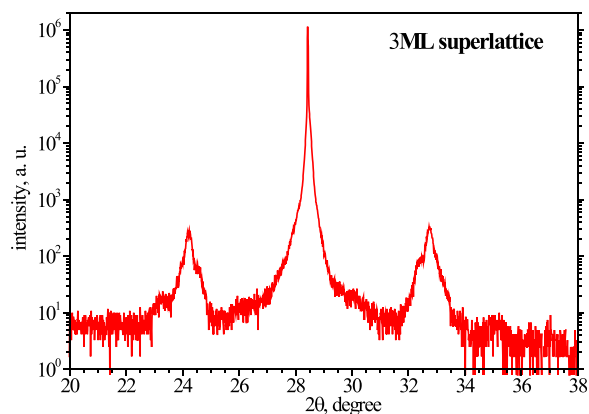
semiconductor properties. In addition, CdF<sub>2</sub> is known to demonstrate an efficient electroluminescence<sup>10,11</sup> and, due to its high density (6.38 g/cm<sup>3</sup>) and relatively fast intrinsic luminescence decay time, can be used as a scintillator.<sup>12,13</sup> CaF<sub>2</sub> is an insulator with very large bandgap estimated to be between 11.8 and 12.1 eV (Refs. 14 and 15) and is widely used in various optical applications.

CdF<sub>2</sub>-CaF<sub>2</sub> SLs and heterostructures are of research interest<sup>8,9,16–18</sup> because of their potential for application in quantum devices such as resonant tunnelling diodes and quantum cascade lasers. This is due to the large (~2.9 eV) conduction band discontinuity of the CdF<sub>2</sub>-CaF<sub>2</sub> interface that was found by means of X-ray photoelectron spectroscopy.<sup>19</sup> Laser spectroscopy of Eu<sup>2+</sup> and Eu<sup>3+</sup> ions doped into CaF<sub>2</sub> MLs of CdF<sub>2</sub>-CaF<sub>2</sub> and defect site distributions for the dopant ions have also been investigated.<sup>20–22</sup>

## II. EXPERIMENTAL

The CaF<sub>2</sub>-CdF<sub>2</sub> SL samples were grown at the Ioffe Institute using molecular beam epitaxy (MBE). A reflection high-energy electron diffractometer (RHEED) was available for *in situ* structural characterization of the growing layers. CaF<sub>2</sub> and CdF<sub>2</sub> layers were sequentially deposited on (111)-oriented Si substrates. The opposite signs of the fluoride lattice mismatches with Si allow pseudomorphic growth of the films with the (111)-plane parallel to the substrate surface. Two samples were used in this work: a 3 ML sample consisting of 50 periods, each period containing 3 MLs of CaF<sub>2</sub> and 3 MLs of CdF<sub>2</sub>, and a 5 ML sample for which the thickness of each fluoride layer was 5 MLs and overall the SL consisted of 30 periods. A CaF<sub>2</sub> monolayer (for example) consists of the electrically neutral triple layer of F<sup>−</sup> - Ca<sup>2+</sup> - F<sup>−</sup> ions. Owing to the fact that the thickness of each fluoride ML was close to 0.315 nm, the total thickness of each superlattice was about 100 nm. The growth procedure is described in more detail in Ref. 8. Fig. 1 shows the  $\theta$ - $2\theta$  double crystal

<sup>a)</sup>Author to whom correspondence should be addressed. Electronic mail: jon-paul.wells@canterbury.ac.nz

FIG. 1. XRD pattern of a 3ML CdF<sub>2</sub>-CaF<sub>2</sub> superlattice structure.

XRD pattern obtained from the 3 ML SL sample. The XRD pattern reveals a well pronounced oscillating structure that suggests reasonably good flatness of the interfaces. The position of the satellite peaks corresponds to a 6 ML period. This result shows that the layered heterostructure has remained free of inter diffusion and/or chemical reaction.

Bulk single crystals of CaF<sub>2</sub> and CdF<sub>2</sub> were grown in a graphite crucible under high vacuum using the vertical Bridgman technique.

The time-resolved VUV spectroscopic measurements were carried out using the SUPERLUMI facility at HASYLAB of DESY (Hamburg, Germany) employing synchrotron radiation (SR) from the DORIS III storage ring as an excitation source (see Ref. 23 and references therein). For selective excitation and measurements of excitation spectra in the range of 3.7–20.4 eV, a 2 m monochromator in a McPherson mounting with a resolution of 3.2 Å was used. The detection of the luminescence and measurement of emission spectra were performed with a 0.3 m ARC SpectraPro-308i monochromator equipped with a high-speed R3809U-50 S (Hamamatsu) microchannel plate (MCP) detector. The time-resolved spectra were recorded within two independent time gates (TGs): 2–9 ns (fast time gate) and 46–70 ns (slow time gate) relative to the beginning of the SR pulse. The time-integrated spectra were recorded counting emission signal within the whole time period of 96 ns available between SR pulses at a 10 bunch mode (BM) of the storage ring. The measurements were performed in the ultra-high-vacuum chamber ( $\sim 10^{-9}$  mbar) in the temperature range of 8–300 K. The excitation spectra were corrected for wavelength-dependent variation of the SR intensity using a sodium salicylate signal. A background signal corresponding to the dark count of the MCP detector was subtracted from the original spectra and decay curves.

X-ray excited emission spectra of CdF<sub>2</sub> and CaF<sub>2</sub> bulk crystals were recorded at Argonne National Lab (US) using BM-20 beamline of the Advanced Photon Source (APS) storage ring. X-rays were delivered via double-crystal Si(111) monochromator (with second crystal detuned 20% from maximum signal) and were focused to a  $500 \times 250 \mu\text{m}$  spot size using a toroidal mirror. For additional rejection of harmonic energies (beyond detuning), a Rh-coated flat mirror was also used. For the measurements of emission spectra, an

Avantes AvaSpec-2048 CCD detector with 300 line/mm grating and a  $50 \mu\text{m}$  slit width (resolution  $\sim 2 \text{ nm}$ ) was used. The spectra were recorded at RT and at low temperatures under vacuum using micro-miniature refrigerator (MMR technologies) based on the Joule-Thomson cooling.

### III. RESULTS AND DISCUSSION

The top panel of Fig. 2 shows the emission spectra of CaF<sub>2</sub> and CdF<sub>2</sub> bulk crystals. Upon excitation with X-ray synchrotron radiation at  $T = 80 \text{ K}$ , the emission spectra of both CaF<sub>2</sub> and CdF<sub>2</sub> bulk crystals are broad emission bands centred near 282 nm (4.40 eV) and 374 nm (3.32 eV), respectively. The spectra did not reveal any noticeable change of shape when the excitation energy was varied from 4 to 10 keV. Moreover, we did not observe any peculiarities in the emission spectra when selectively excited into or just above the Ca K core level (4038 eV) or Cd L<sub>α1</sub> core level (4018 eV).

The emission observed from CaF<sub>2</sub> is due to radiative recombination of self-trapped excitons (STE).<sup>24</sup> The emission band is only slightly broadened at  $T = 300 \text{ K}$  relative to that at

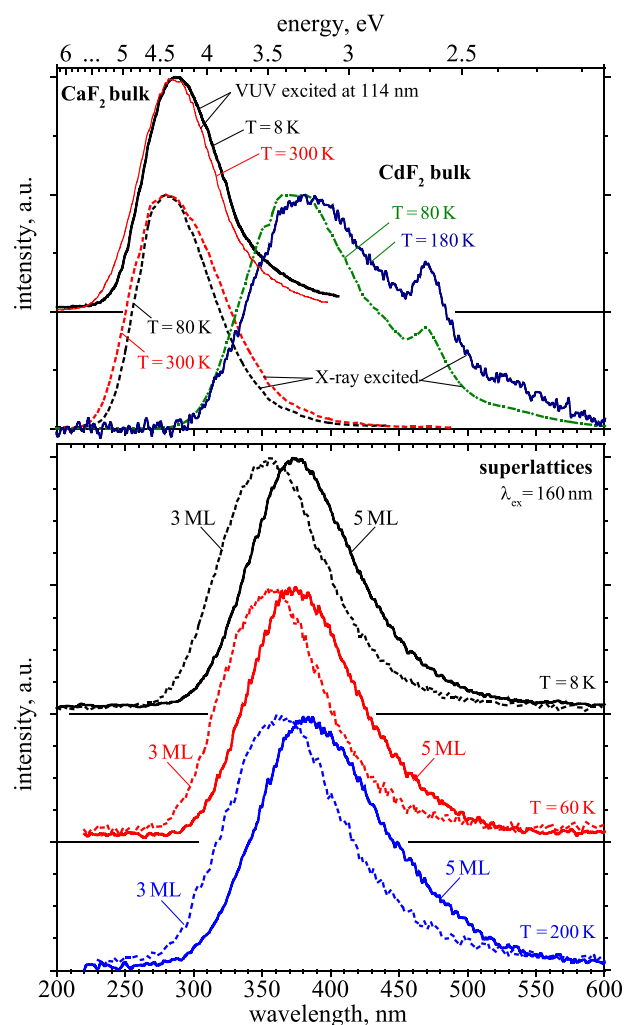


FIG. 2. Time integrated emission spectra of the CdF<sub>2</sub>-CaF<sub>2</sub> superlattices recorded upon VUV excitation at 8, 60, and 200 K (bottom panel) and CdF<sub>2</sub> and CaF<sub>2</sub> bulk crystals recorded upon VUV and X-ray excitation at 8, 80 and 180 K (upper panel).

$T = 80$  K. The STE emission observed in  $\text{CaF}_2$  can also be observed in time-integrated emission spectra recorded upon VUV excitation at 114 nm (10.9 eV)—corresponding to the peak excitonic absorption (Fig. 2, top panel). A slight ( $\sim 0.03$  eV) blue shift of the band maxima at 300 K is due to the quenching of the emission arising from the excitonic singlet state which occurs at slightly lower energy.

The width and maximum of the emission band observed for  $\text{CdF}_2$  upon X-ray excitation are in good agreement with data published in Refs. 25–28. The peak at 470 nm (2.63 eV) is an experimental artifact that is typically observed in spectra of samples where the measured luminescence is weak. The X-ray excited emission of  $\text{CdF}_2$  is entirely quenched above sample temperatures of 200 K. We note that the intrinsic emission in  $\text{CdF}_2$  is not well understood with various studies assigning the 374 nm emission as electron-self trapped hole recombination<sup>25</sup> or exciton recombination.<sup>28</sup>

The bottom panel of Fig. 2 shows the time-integrated emission spectra of 5 ML and 3 ML  $\text{CdF}_2$ - $\text{CaF}_2$  superlattices recorded upon excitation at 160 nm (7.75 eV) at temperatures 8, 60, and 200 K. At  $T = 8$  K, the spectra are represented by broad asymmetric emission bands peaked at 354 nm (3.50 eV) and 375 nm (3.31 eV), for the 3 ML and 5 ML superlattices, respectively. The FWHM of the emission bands for both the 3 ML and 5 ML superlattices at  $T = 8$  K is approximately 0.76 eV. The intensity of the emission is observed to dramatically decrease with temperature. For temperatures above 200 K, the emission was very weak and a reliable emission spectrum could not be recorded. Both the 5 ML and 3 ML superlattices exhibit a shift of the emission band maxima towards lower energy close to 0.1 eV as well as a 15% band broadening as the temperature increases from 8 to 200 K. Spectra recorded within slow and fast time gates closely follow the time-integrated spectra (not shown).

No emission could be detected from any of the available superlattice samples upon X-ray excitation at temperatures above 80 K. The position of the emission peaks in the 3 ML and 5 ML superlattice structures as well as the  $\text{CdF}_2$  and  $\text{CaF}_2$  bulk crystals at different temperatures and for different excitation wavelengths is given in Table I along with data on

the fundamental absorption edge. The superlattice emission spectra are closely comparable with that of bulk  $\text{CdF}_2$  and do not show any noticeable variation as the excitation energy is increased from 8 eV to 21 eV, the upper limit going well past the fundamental absorption edge of  $\text{CaF}_2$ . Thus, the STE emission of  $\text{CaF}_2$  is quenched within the superlattice structures and the emission spectra are entirely dominated by excitonic recombination within the  $\text{CdF}_2$  layers.

Temperature dependent, time-integrated and time-resolved excitation spectra recorded monitoring the  $\text{CdF}_2$  exciton emission in the 3 ML and 5 ML superlattices are shown in the bottom panel of Fig. 3. At  $T = 8$  K, both the 3 ML and 5 ML samples demonstrate similar excitation spectra. In particular, the spectra reveal an absorption onset at about 6.8 eV and an excitonic-like peak at about 7.7 eV which is followed by a gradual decrease of intensity to essentially background level when the energy of the exciting photons reaches around 13 and 14 eV for 3 ML and 5 ML samples, respectively. At energies higher than 17 eV, the signal is observed to increase. At  $T = 8$  K, the spectra recorded within fast and slow time gates closely follow those recorded in time-integrated mode. However, the temperature dependencies of the excitation spectra are quite different for the two samples. The excitation spectra of the 3 ML sample show a signal increase near 21 eV as the temperature increases up to 200 K, while the spectra of 5 ML sample show the development of intense broad excitation structure above 8.5 eV (Fig. 3, bottom right panel) which appears to peak near 21 eV. This is accompanied by an increase in intensity within the slow time gated excitation spectra. At  $T = 200$  K, the time-integrated spectrum of the 5 ML superlattice appears as a continuous band.

The top panels of Fig. 3 show the excitation and reflection spectra of  $\text{CdF}_2$  and  $\text{CaF}_2$  single crystals for comparison with the excitation spectra of the superlattice samples. The time-integrated excitation spectrum for the  $\text{CaF}_2$  crystal was recorded at a sample temperature 8 K while monitoring STE emission at  $\lambda = 287$  nm (4.32 eV). Reflection spectra for both the  $\text{CdF}_2$  and  $\text{CaF}_2$  crystals as well as the excitation spectrum obtained monitoring the  $\text{CdF}_2$  exciton emission (all

TABLE I. Exciton emission and fundamental absorption edge observed in  $\text{CaF}_2$ - $\text{CdF}_2$  superlattices and  $\text{CaF}_2$  and  $\text{CdF}_2$  bulk crystals. All measurements are given in units of eV.

	CaF <sub>2</sub> -CdF <sub>2</sub> superlattice					Bulk crystal				
	T (K)	5 ML		3 ML		T (K)	CdF <sub>2</sub>		CaF <sub>2</sub>	
		Exc.		Exc.			Exc.		Exc.	
Emission peak (eV)	8	VUV	3.32	VUV	3.50	8	...		VUV	4.32
	60		3.31		3.47	80	X-ray	3.32		...
							VUV	3.51 <sup>a</sup>		
	200		3.22		3.41	180	X-ray	3.22		
Fundam. absorption edge (eV)	300		quenched		quenched	300	X-ray	3.18 <sup>b</sup>	VUV	4.35
	8		7.43		7.45	8	...			10.72
	100		7.42		7.42	~80	6.6 <sup>b</sup>			10.68
	200		7.35		7.31					
	300		Quenched		Quenched	300	...			10.29

<sup>a</sup>Reference 26.

<sup>b</sup>Reference 29.

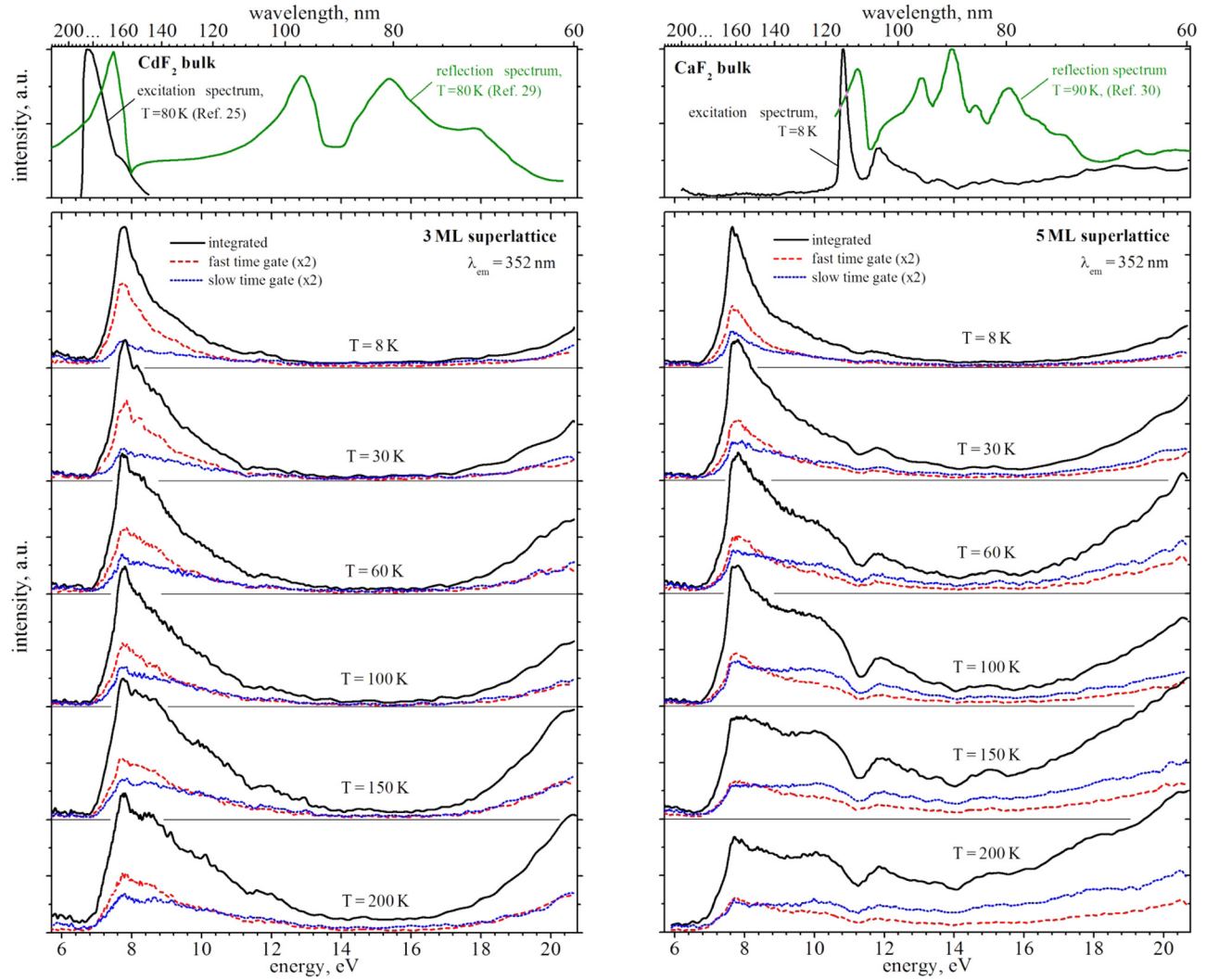


FIG. 3. Excitation spectra of the CdF<sub>2</sub>-CaF<sub>2</sub> superlattices recorded in the temperature range 8–200 K by monitoring emission at  $\lambda_{\text{em}} = 355$  nm and  $\lambda_{\text{em}} = 375$  nm for 3 ML and 5 ML superlattices, respectively. The top panels show excitation and reflection spectra obtained for CaF<sub>2</sub> and CdF<sub>2</sub> bulk crystals.

measured at liquid nitrogen temperature) were extracted from published sources<sup>14,26,30</sup> using graph digitizing software.

Table I compares the energies of the fundamental absorption edge in the CaF<sub>2</sub>-CdF<sub>2</sub> superlattices with that of the CdF<sub>2</sub> and CaF<sub>2</sub> bulk crystals. The datum point is taken at half intensity on the low-energy side of the band edge (excitonic) peak. The onset of the fundamental absorption of the superlattice samples is located at about 0.8–0.85 eV higher energy relative to that observed for the CdF<sub>2</sub> bulk crystal. We note that the position of the band edge peak in the excitation spectrum of the CdF<sub>2</sub> bulk crystal from Ref. 25 agrees well with the position of the first maximum of the reflection spectrum observed at 7.5–7.6 eV (Refs. 30, 31, and 32) which corresponds to an excitonic transition at the  $\Gamma$  point as confirmed by theoretical calculations.<sup>33</sup> The excitation spectrum of the CaF<sub>2</sub> bulk crystal taken at T = 8 K exhibits an intense excitonic peak with an intensity maximum at 10.8 eV which is followed by dramatic decrease of intensity at about 11.3 eV which corresponds to the first maximum in the reflection spectrum (as shown in Fig. 3) and very high absorption coefficient.

At T = 8 K, the excitonic peak in the excitation spectra of the superlattices is followed by a gradual absorption

decrease up to about 13.5–14 eV that can be explained in terms of migration losses which occur because the increased kinetic energy of electrons and holes created via interband excitation increases their probability for escape from the sphere of effective *e-h* interactions.<sup>34,35</sup>

In Fig. 3, we also show an excitation spectrum for STE emission in a CaF<sub>2</sub> bulk crystal that helps one to see that the excitation spectra of the superlattices do not show any features that could indicate an energy transfer from electronic excitations occurred in CaF<sub>2</sub> MLs. This fact together with the above-mentioned peculiarities of the emission spectra suggests the VUV photons are substantially absorbed in CdF<sub>2</sub> MLs. A dip observed near 11.26 eV in all the excitation spectra of the superlattice samples is probably related to reflection losses in the CaF<sub>2</sub> MLs.

It is also worth noting that the excitonic peak in the bulk CdF<sub>2</sub> spectrum is quite broad compared to that observed in the bulk CaF<sub>2</sub> spectrum. This comes from the fact that the binding energy of the CdF<sub>2</sub> exciton ( $\sim 1.75$  eV (Ref. 6)) is almost double that of the CaF<sub>2</sub> exciton (0.94 eV (Ref. 36)). A greater binding energy indicates a greater configurational shift and broader emission band. The increase in intensity of



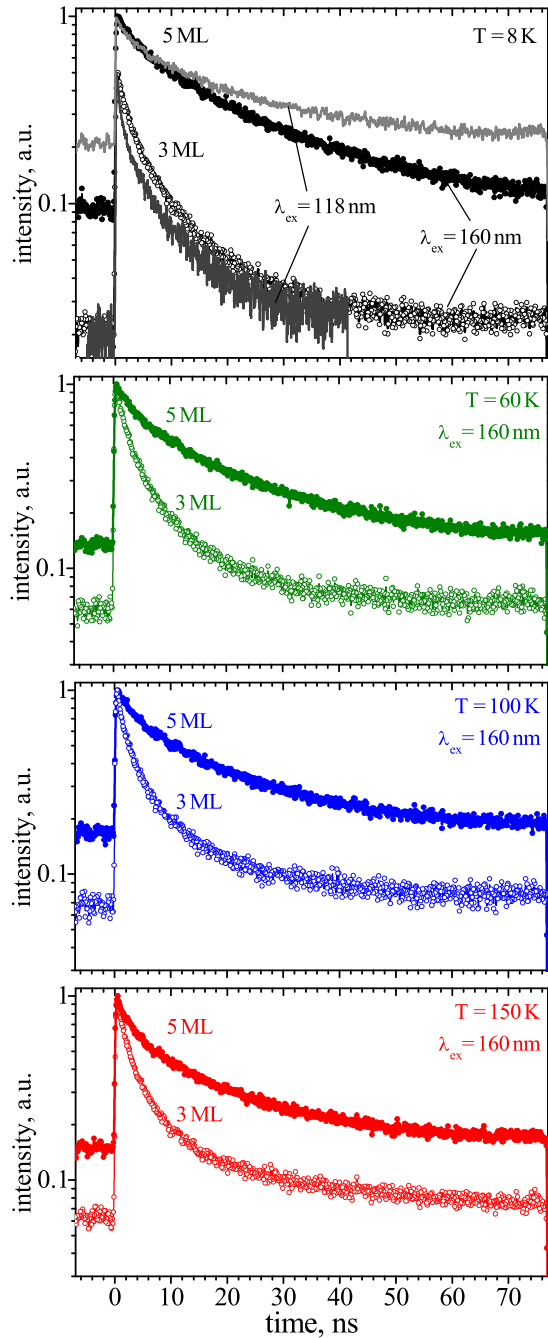


FIG. 4. Emission decay kinetics of CdF<sub>2</sub>-CaF<sub>2</sub> superlattices recorded upon excitation at  $\lambda_{\text{ex}} = 160$  nm in temperature range 8–150 K.

the excitation spectrum of the CdF<sub>2</sub> exciton emission observed above 16.5 eV is probably connected with photon multiplication. We note that CdF<sub>2</sub> is characterised by a broad valence band ( $E_{\text{VB}} > E_g$ ),<sup>37</sup> which implies that the generation of secondary electronic excitations may be induced by both high-energy primary electrons and holes.

Fig. 3 shows the luminescence decay curves for the CdF<sub>2</sub> exciton in SLs recorded upon excitation at 7.7 eV which demonstrate a departure from the exponential behaviour that is most pronounced for 3 ML sample.

Emission from the self-trapped exciton has been previously assigned to three states in alkali halides.<sup>37</sup> A long  $\pi$  recombination has been identified with a lifetime of several

ms and assigned to a mix of B<sub>2g</sub>, B<sub>1u</sub>, and B<sub>2u</sub> states of the M<sub>2</sub>X<sub>2</sub> alkali halide molecule. Two fast recombinations with lifetimes of nanoseconds and  $\sigma$  polarisation are suggested to be from a mix of B<sub>2g</sub> and B<sub>3u</sub> states which have different spin multiplicities. These three emission components can be fitted to the transients in Fig. 4 by fitting two exponential functions for the  $\sigma$  components with an offset to represent the long  $\pi$  recombination.

The fitting parameters for the decay transients recorded from superlattices are given in Table II. The values of lifetimes obtained are much shorter than those documented in Ref. 28 for the CdF<sub>2</sub> bulk crystal, where the fastest decay component observed for CdF<sub>2</sub> emission was about 18 ns at room temperature and of order of 1  $\mu$ s for liquid N<sub>2</sub> temperature. Moreover, we do not observe any significant dependence of lifetime on temperature in contrast to the CdF<sub>2</sub> bulk crystal.<sup>28</sup>

The decay components are around twice as fast for the 3 ML than for 5 ML sample and the amplitude (and fraction) of the fast decay component is greater for the 3 ML sample. For the 3 ML sample, the long lifetime does not appreciably change with temperature, while the short lifetime decreases slightly. For the 5 ML sample, both lifetimes decrease with temperature. The offset increases with temperature for both samples, which agrees with the observation that for alkali halides the  $\sigma$  components of the decay are quenched at a lower temperature than the  $\pi$  component.<sup>38</sup>

The observed spectroscopic and dynamic properties suggest that relaxation processes in the CdF<sub>2</sub>-CaF<sub>2</sub> superlattices are strongly influenced by quantization effects arising since the confinement length is comparable to the Bohr radius. A decrease in the lifetime of excitonic emission in 1D materials has previously been attributed to quantum confinement effects,<sup>39</sup> while excitonic confinement effects are routinely observed for semiconductor quantum dots and thin films.<sup>40,41</sup>

It is well known that the creation of excitons in alkali-earth fluorides begins from picosecond relaxation of (hot) holes which leads to the formation of self-trapped holes or V<sub>k</sub>-centres. The V<sub>k</sub> centres can capture electrons and form weakly bonded electron-hole pairs before relaxing into a STE (off-centre exciton). According to Ref. 42, such states can have an on-centre configuration of the exciton with the electron localized in vicinity of the V<sub>k</sub>-centre. The Bohr radius of such a high energy (non-relaxed) exciton can be of the order of several lattice constants. Thus, considering the superlattices, it is reasonable to expect confinement effects to be significant for quantum wells which are 5 MLs thick or smaller.

The confinement effect in SLs is readily observable in excitation spectra via the blue shift of the CdF<sub>2</sub> excitonic peak relative to those in bulk crystal (see Table I). The blue shift of the exciton emission band is less obvious. This is consistent with the smaller Bohr radius (nearly one lattice constant) of the self-trapped (relaxed) exciton.

#### IV. CONCLUSIONS

We have utilised VUV and X-ray synchrotron sources to investigate the high energy elementary excitations in CdF<sub>2</sub>-

TABLE II. Parameters fitted to the  $\text{CaF}_2\text{-CdF}_2$  superlattice emission transients.

T (K)	8 K	60 K	100 K	150 K
3 ML				
Amplitude $A_1$	$0.63 \pm 0.02$	$0.732 \pm 0.015$	$0.77 \pm 0.02$	$0.725 \pm 0.015$
Lifetime $\tau_1$ (ns)	$1.84 \pm 0.010$	$1.76 \pm 0.13$	$1.60 \pm 0.07$	$1.60 \pm 0.06$
Amplitude $A_2$	$0.46 \pm 0.02$	$0.39 \pm 0.02$	$0.35 \pm 0.02$	$0.36 \pm 0.02$
Lifetime $\tau_2$ (ns)	$9.0 \pm 0.3$	$8.6 \pm 0.3$	$9.4 \pm 0.4$	$9.0 \pm 0.6$
Offset $y_0$	$0.0500 \pm 0.0008$	$0.0674 \pm 0.0018$	$0.0799 \pm 0.0009$	$0.0815 \pm 0.0008$
5 ML				
Amplitude $A_1$	$0.32 \pm 0.02$	$0.35 \pm 0.02$	$0.36 \pm 0.03$	$0.38 \pm 0.02$
Lifetime $\tau_1$ (ns)	$3.2 \pm 0.3$	$3.3 \pm 0.3$	$3.0 \pm 0.3$	$2.5 \pm 0.2$
Amplitude $A_2$	$0.62 \pm 0.003$	$0.56 \pm 0.02$	$0.54 \pm 0.02$	$0.48 \pm 0.02$
Lifetime $\tau_2$ (ns)	$20.4 \pm 0.5$	$19.2 \pm 0.6$	$18.6 \pm 0.7$	$16.5 \pm 0.5$
Offset $y_0$	$0.103 \pm 0.003$	$0.144 \pm 0.002$	$0.179 \pm 0.003$	$0.167 \pm 0.002$

$\text{CaF}_2$  superlattices. It is observed that the luminescence spectroscopic properties of these materials are largely governed by the behaviour of the  $\text{CdF}_2$  quantum well (3 and 5 ML thick in our samples) due to its smaller band gap. Excitonic emission in the  $\text{CdF}_2\text{-CaF}_2$  superlattices was detectable for temperatures below 200 K. Excitation spectra recorded monitoring excitonic emission reveals a significant (up to 0.85 eV) blue shift of the  $\text{CdF}_2$  fundamental absorption that is related to confinement of non-relaxed (high energy) excitons. In addition, for the both 3 and 5 ML superlattices confinement effects are well pronounced in emission spectra and luminescence decay transients.

## ACKNOWLEDGMENTS

This work was supported by the Marsden fund of the Royal Society of New Zealand via Grant No. 09-UOC-080. R.B.H.C. acknowledges support from the University of Canterbury via a doctoral scholarship. K.V.I. acknowledges partial support via the UrfU Competitiveness Enhancement Program. Sector 20 operations of the APS are supported by the U.S. Department of Energy and the Canadian Light Source, with additional support from the University of Washington. E. Radzhabov (Vinogradov Institute of Geochemistry, Russia) is acknowledged for providing us with  $\text{CdF}_2$  crystal.

- <sup>1</sup>R. Dingle, W. Wiegmann, and C. H. Henry, *Phys. Rev. Lett.* **33**, 827 (1974).
- <sup>2</sup>J. Hegarty, L. Goldner, and M. D. Sturge, *Phys. Rev. B* **30**, 7346 (1984).
- <sup>3</sup>A. Schülzgen, R. Binder, M. E. Donovan, M. Linberg, K. Wundke, H. M. Gibbs, G. Khitrova, and N. Peyghambarian, *Phys. Rev. Lett.* **82**, 2346 (1999).
- <sup>4</sup>J. Brown, J.-P. R. Wells, D. O. Kundy, A. M. Fox, T. Wang, P. J. Parbrook, D. J. Mowbray, and M. S. Skolnick, *J. Appl. Phys.* **104**, 053523 (2008).
- <sup>5</sup>C. Klingshim, "Spectroscopy of quantum wells and superlattices," in *Frontiers of Optical Spectroscopy*, edited by B. Bartolo and O. Forte (Springer, Netherlands, 2005), pp. 221–250.
- <sup>6</sup>M. H. Yang and C. P. Flynn, *Phys. Rev. B* **41**, 8500 (1990).
- <sup>7</sup>S. Sinharoy, *Thin Solid Films* **187**, 231 (1990).
- <sup>8</sup>N. S. Sokolov and S. M. Surtin, *Appl. Surf. Sci.* **175–176**, 619 (2001).
- <sup>9</sup>N. S. Sokolov, S. V. Gastev, A. Y. Khilko, R. N. Kyutt, S. M. Surtin, and M. V. Zamoryanskaya, *J. Cryst. Growth* **201–202**, 1053 (1999).
- <sup>10</sup>C. Paracchini and G. Schianchi, *Solid State Commun.* **21**, 1107 (1977).

- <sup>11</sup>J. M. Langer, T. Langer, and B. Krukowska-Fulde, *J. Phys. D: Appl. Phys.* **12**, L95 (1979).
- <sup>12</sup>R. V. Jones and J. H. Pollard, *Proc. Phys. Soc.* **79**, 358 (1962).
- <sup>13</sup>M. Ishii and M. Kobayashi, *Prog. Cryst. Growth Charact.* **23**, 245 (1992).
- <sup>14</sup>G. W. Rubloff, *Phys. Rev. B* **5**, 662 (1972).
- <sup>15</sup>E. L. Shirley, *Phys. Rev. B* **58**, 9579 (1998).
- <sup>16</sup>T. Kanazawa, R. Fujii, T. Wada, Y. Suzuki, and M. Watanabe, *Appl. Phys. Lett.* **90**, 092101 (2007).
- <sup>17</sup>K. Jinen, T. Kikuchi, M. Watanabe, and M. Asada, *Jpn. J. Appl. Phys. Part 1* **45**, 3656 (2006).
- <sup>18</sup>N. S. Sokolov, S. V. Gastev, A. Y. Khilko, S. M. Surtin, I. N. Yassievich, J. M. Langer, and A. Kozanecki, *Phys. Rev. B* **59**, R2525 (1999).
- <sup>19</sup>A. Izumi, Y. Hirai, K. Tsutsui, and N. S. Sokolov, *Appl. Phys. Lett.* **67**, 2792 (1995).
- <sup>20</sup>R. J. Reeves, J. K. Choi, S. V. Gastev, A. V. Krupin, K. R. Hoffman, and N. S. Sokolov, *J. Alloys Compd.* **451**, 84 (2008).
- <sup>21</sup>S. M. Surtin, S. A. Basun, S. V. Gastev, J. M. Langer, R. S. Meltzer, and N. S. Sokolov, *Appl. Surf. Sci.* **162–163**, 474 (2000).
- <sup>22</sup>G. A. Valkovskiy, M. V. Durnev, M. V. Zamoryanskaya, S. G. Konnikov, A. V. Krupin, A. V. Moroz, N. S. Sokolov, A. N. Trofimov, and M. A. Yagovkina, *Phys. Solid State* **55**, 1498 (2013).
- <sup>23</sup>G. Zimmerer, *Radiat. Meas.* **42**, 859 (2007).
- <sup>24</sup>R. B. Hughes-Currie, A. J. Salkeld, K. V. Ivanovskikh, M. F. Reid, J.-P. R. Wells, and R. J. Reeves, *J. Lumin.* **158**, 197 (2015).
- <sup>25</sup>S. Benci and G. Schianchi, *J. Lumin.* **11**, 349 (1976).
- <sup>26</sup>F. Fermi, C. Paracchini, and N. Zema, *J. Lumin.* **31–32**, 108 (1984).
- <sup>27</sup>A. Tzalmuna, *J. Phys. Soc. Jpn.* **34**, 1108 (1973).
- <sup>28</sup>E. Radzhabov and R. Shendrik, *IEEE Trans. Nucl. Sci.* **61**, 402 (2014).
- <sup>29</sup>P. A. Rodnyi, I. V. Khodyuk, and G. B. Stryganyuk, *Phys. Solid State* **50**, 1639 (2008).
- <sup>30</sup>C. Raisin, J. M. Berger, and S. Robin-Kandare, *J. Phys. C: Solid State Phys.* **13**, 1835 (1980).
- <sup>31</sup>R. A. Forman, W. R. Hosler, and R. F. Blunt, *Solid State Commun.* **10**, 19 (1972).
- <sup>32</sup>A. J. Bourdillon and J. H. Beaumont, *J. Phys. C: Solid State Phys.* **9**, L473 (1976).
- <sup>33</sup>A. I. Kalugin and V. V. Sobolev, *Phys. Rev. B* **71**, 115112 (2005).
- <sup>34</sup>V. V. Mikhailin, *Nucl. Instrum. Methods Phys. Res. A* **261**, 107 (1987).
- <sup>35</sup>A. N. Belsky and J. C. Krupa, *Displays* **19**, 185 (1999).
- <sup>36</sup>S. Emura, T. Moriga, J. Takizawa, M. Nomura, K. R. Bauchspiess, T. Murata, K. Harada, and H. Maeda, *Phys. Rev. B* **47**, 6918 (1993).
- <sup>37</sup>E. Cadelano and G. Cappellini, *Eur. Phys. J. B* **81**, 115 (2011).
- <sup>38</sup>I. M. Blair, D. Pooley, and D. Smith, *J. Phys. C: Solid State Phys.* **5**, 1537 (1972).
- <sup>39</sup>T. Takagahara and K. Takeda, *Phys. Rev. B* **46**, 15578 (1992).
- <sup>40</sup>G. D. Scholes and G. Rumbles, *Nat. Mater.* **5**, 683 (2006).
- <sup>41</sup>A. A. Mosquera, D. Horwat, A. Rashkovskiy, A. Kovalev, P. Miska, D. Wainstein, J. M. Albella, and J. L. Endrino, *Sci. Rep.* **3**, 1714 (2013).
- <sup>42</sup>K. Tanimura, *Phys. Rev. B* **63**, 184303 (2001).